Quantifying source and sink habitats and pathways in spatially structured populations: a generalized modelling approach

Christine Sample[a], Joanna A. Bieri[b], Benjamin Allen[a,c], Yulia Dementieva[a], Alyssa Carson[a], Connor Higgins[a], Sadie Piatt[a], Shirley Qiu[a], Summer Stafford[b], Brady J. Mattsson[d], Darius J. Semmens[e], Wayne E. Thogmartin[f], Jay E. Diffendorfer[e]

[a]*Department of Mathematics, Emmanuel College, Boston, MA, USA*
[b]*Department of Mathematics and Computer Science, University of Redlands, Redlands, CA, USA*
[c]*Program for Evolutionary Dynamics, Harvard University, Cambridge MA, USA*
[d]*Institute of Wildlife Biology and Game Management, University of Natural Resources and Life Sciences, Vienna, Austria*
[e]*U.S. Geological Survey Geosciences and Environmental Change Science Center, Denver, CO, USA*
[f]*U.S. Geological Survey Upper Midwest Environmental Sciences Center, La Crosse, WI, USA*

Abstract

The ability to classify habitats and movement pathways as sources or sinks is an important part of the decision making process for the conservation of spatially structured populations. Diverse approaches have been used to quantify the importance of habitats and pathways in a spatial network; however, these approaches have been limited by a lack of general applicability across life histories and movement strategies. In this paper, we develop a generalized per-capita contribution metric, the C-metric, for quantifying habitat and pathway quality. This metric is novel in that it can be applied broadly to both metapopulations and migratory species. It allows for any number of age and sex classes, unlimited number of seasons or time intervals within the annual cycle, and for density-dependent parameters. We demonstrate the flexibility of the metric with four case studies: a hypothetical metapopulation, elk of the Greater Yellowstone Ecosystem, northern pintail ducks in North America, and the eastern

Email address: samplec@emmanuel.edu (Christine Sample)

population of the monarch butterfly. General computer code to calculate the per-capita contribution metric is provided. We demonstrate that the C-metric is useful for identifying source and sink habitats in a network and suggest that the C-metric could be supplemented by some measure of network structure for a more robust description of habitat or pathway importance.

Keywords: migration, network model, habitat quality, spatial ecology, metric, ecological traps

---

1. Introduction

Understanding the movement of individuals across space and time is fundamental to making management decisions. Migratory species, and some species showing metapopulation dynamics, can be difficult to conserve and manage because they use multiple habitat types across geographies that span political boundaries (Behrens et al., 2008; Wilcove and Wikelski, 2008; Visser et al., 2009; Runge et al., 2017; Tucker et al., 2018). A crucial part of developing conservation strategies for such species is assessing the relative importance of the habitats they occupy over the course of their full annual cycle (Martin et al., 2007; Kölzsch and Blasius, 2008; Sawyer and Kauffman, 2011). It is therefore worth developing metrics that account for both habitat connectivity and demography (Johnson et al., 2018; Robertson et al., 2018; Zamberletti et al., 2018). Although several habitat contribution metrics exist for spatially structured populations (Nicol et al., 2016), these metrics were not designed to account for seasonal migration. Applying these metrics to a migratory population can therefore be problematic.

Recently, several approaches have been developed to address the question of habitat importance for migratory populations. The metric C^r, originally developed by Runge et al. (2006) for non-migratory but spatially structured populations, is the per-capita contribution to the next generation by individuals that occur in a particular habitat r. Wiederholt et al. (2018) adapted this per-capita contribution metric for migratory species, which accounts for seasonal

movement between multiple breeding and non-breeding habitats and for both resident and migratory cohorts. This metric, however, is limited to a two-season population of juveniles and adults. Erickson et al. (2018) considered per-capita contribution metrics for a migratory network but only for the case of a single class of individuals.

The usefulness of per-capita contribution metrics is that they allow managers to compare habitat (node) and pathway (edge) values and thus compare locations and routes across an entire migratory network for a species. Nodes and edges can be classified as sources or sinks (Erickson et al., 2018) and prioritized for management actions based on their relative values. The relative importance of different habitats has also been used to spatially allocate the value of ecosystem services provided by migratory species (Semmens et al., 2011, 2018). Although per-capita contribution metrics have been recognized as important tools for understanding dynamics of spatially structured populations, until now there has been no generalized method that accounts for the full range of life history strategies.

In this paper, we generalize an existing per-capita contribution metric (Wiederholt et al., 2018), which we will refer to as the C-metric. The C-metric is novel in that it can be applied to any number of seasons, non-equal season lengths, varied class structures, and the full range of movement strategies. We illustrate the C-metric by applying our model to four example species. The first is a simple hypothetical metapopulation for demonstrating the calculation and illustrating that the metric can be applied to non-migratory metapopulations. We then apply the metric to existing models (Sample et al., 2018) of a partially migratory population (*Cervus canadensis*; elk), a complete migratory population (*Anas acuta*; northern pintail), and a population exhibiting a stepping stone migration strategy (*Danaus plexippus*; monarch butterflies). These cases represent a diversity of age and stage structures along with alternate types of migration. Our generalization, which relies on mathematics from matrix algebra, includes general R code for calculating the C-metric to more easily allow use by managers and decision makers (Bieri et al., 2019). We draw several new

insights about population dynamics revealed in each of the case studies.

Network Structure and Demographic Parameters and Variables	
Symbol	Definition
c	number of classes (life stages)
n	number of nodes in the network
s	number of seasons in the annual cycle
t	time variable; one time step, $t+1$, represents one season, and $t+s$ represents one annual cycle
$N_{i,t}^{x}$	population size of class x in node i at time t
N_{t}^{tot}	total network population size at time t, $N_{t}^{tot} = \sum_{i=1}^{n} \sum_{x=1}^{c} N_{i,t}^{x}$
$f_{i,t}^{xy}$	proportion of individuals in class x that transition to class y at node i and time t, element of $\mathbf{F}_{i,t}$
$p_{ij,t}^{x}$	proportion of individuals of class x that move from node i to node j at time t
$s_{ij,t}^{x}$	proportion of individuals of class x that survive the transition from node i to node j at time t
$q_{ij,t}^{x}$	proportion of individuals of class x that move, and survive the movement, from node i to node j at time t, $q_{ij,t}^{x} = p_{ij,t}^{x} s_{ij,t}^{x}$ are elements of matrix $\mathbf{Q}_{t}^{x}$
λ_t	annual growth rate of the network at time t

Table 1: Symbols used in the paper.

Contribution Metric Variables	
Symbol	Definition
$\vec{\mathbf{C}}_t$	block vector of per-capita habitat contributions, whose elements are $C^x_{r,t}$, eq. (8)
$C^x_{r,t}$	annual per-capita contribution of an individual of class x starting at node r and time t
$C_{r,t}$	class population-weighted average of annual habitat per-capita contribution, eq. (9)
$\bar{C}_r$	class and seasonal population-weighted average of annual habitat per-capita contribution, eq. (10)
$C^x_{rd,t}$	annual per-capita contribution of an individual of class x using pathway rd at time t
$C_{rd,t}$	class population-weighted average of annual pathway per-capita contribution, eq. (12)
$\bar{C}_{rd}$	class and seasonal population-weighted average of annual pathway per-capita contribution, eq. (13)

Table 2: Symbols used in the paper.

Annual Projection Matrices and Vectors	
Symbol	Definition
$\mathbf{A}_t$	$nc \times nc$ projection matrix that contains demographic and movement information, $\mathbf{A}_t = \mathbb{Q}_t\mathbb{F}_t$
$\mathbb{F}_t$	$nc \times nc$ block matrix that contains demographic information at the nodes
$\mathbf{F}_{i,t}$	$c \times c$ demographic projection matrix for node i
$\mathbb{Q}_t$	$nc \times nc$ block matrix that contains movement and survival probabilities along pathways
$\mathbf{Q}_t^x$	$n \times n$ movement and pathway survival matrix for class x
$\hat{\mathbf{A}}_t$	$nc \times nc$ matrix that projects the population over one annual cycle, $\hat{\mathbf{A}}_t = A_{t+s-1} \cdots A_{t+1}A_t$
$\vec{\mathbf{N}}_{i,t}$	$c \times 1$ vector of population size for each class at node i
$\vec{\mathbf{N}}_t$	$nc \times 1$ block vector of population sizes, whose subvectors are $\vec{\mathbf{N}}_{i,t}$
$\vec{\mathbf{w}}_t$	$1 \times nc$ vector of population proportions, $\vec{\mathbf{w}}_t = \vec{\mathbf{N}}_t^T / N_t^{tot}$
$\mathbf{I}_{nc}$	$nc \times nc$ identity matrix
$\mathbf{1}_n$	$n \times n$ matrix of ones
$\vec{\mathbf{1}}_{nc}$	$nc \times 1$ vector of ones
$\mathbf{E}_{n,rd}$	$n \times n$ matrix of zeros with a 1 at position rd
$\mathbf{H}_{c,x}$	$c \times c$ zero matrix with ones in column x

Mathematical Operators	
Symbol	Definition
$\otimes$	Kronecker matrix product
$\circ$	Hadamard (entrywise) matrix product
T	as a superscript, the transpose of a vector or matrix

Table 3: Symbols used in the paper.

2. Materials and Methods

Borrowing from the matrix population models that are used widely to study age and size-structured populations (Rogers, 1966; Pascarella and Horvitz, 1998; Caswell, 2001; Hunter and Caswell, 2005), we construct a time-dependent projection matrix, $\mathbf{A}_t$, that contains the demographic and movement information required to calculate the C-metric. In doing so, we represent the spatial structure of a population as a network in which habitats are nodes and movement pathways are edges (Taylor and Norris, 2010; Sample et al., 2018). Symbols used throughout this paper are given in Tables 1 - 3.

We consider a population of c age classes (or life stages) in a network of n nodes and s seasons. Individuals are classified by both their class and location. One time step, from t to $t+1$, represents one season in the annual cycle (seasons do not have to be equal in duration), and s time steps, from t to $t+s$, represents one year. We define $\mathbf{A}_t$ as an $nc \times nc$ matrix that projects the population, in all classes and nodes, from one time step to the next. Each entry in $\mathbf{A}_t$ gives the probability that an individual in a given node and class at time t will contribute to that class or become another class in the same or another node, by time $t+1$. To ease the construction of this matrix, we write it as the product of two matrices:

$$\mathbf{A}_t = \mathbb{Q}_t \mathbb{F}_t. \tag{1}$$

The block matrix $\mathbb{F}_t$ contains demographic update information at the nodes (such as fecundity, class transition, and survival rates; see eqs. (2) and (3) below), and block matrix $\mathbb{Q}_t$ contains update information along the pathways (such as movement and survival probabilities; see eqs. (4) and (5) below). $\mathbb{F}_t$ is defined as

$$\mathbb{F}_t = \sum_{i=1}^{n} \mathbf{E}_{n,ii} \otimes \mathbf{F}_{i,t}^T, \tag{2}$$

where $\otimes$ represents the Kronecker product, $\mathbf{E}_{n,ii}$ is an $n \times n$ zero matrix with

a 1 at position ii, and $\mathbf{F}_{i,t}$ is a $c \times c$ demographic projection matrix for node i,

$$\mathbf{F}_{i,t} = \begin{pmatrix} f_{i,t}^{11} & f_{i,t}^{12} & \cdots & f_{i,t}^{1c} \\ f_{i,t}^{21} & f_{i,t}^{22} & \cdots & f_{i,t}^{2c} \\ \vdots & \cdots & \ddots & \vdots \\ f_{i,t}^{c1} & \cdots & \cdots & f_{i,t}^{cc} \end{pmatrix}. \tag{3}$$

Element $f_{i,t}^{xy}$ represents individuals transitioning from class x to class y at node i and time t, and $f_{i,t}^{xx}$ represents individuals remaining in class x. These elements may be given as survival probabilities, and may also include births so their values may be greater than 1. Matrix $\mathbb{Q}_t$ is defined as

$$\mathbb{Q}_t = \sum_{x=1}^{c} (\mathbf{Q}_t^x)^T \otimes \mathbf{E}_{c,xx}, \tag{4}$$

where $\mathbf{Q}_t^x$ is an $n \times n$ movement matrix,

$$\mathbf{Q}_t^x = \begin{pmatrix} q_{11,t}^x & q_{12,t}^x & \cdots & q_{1n,t}^x \\ q_{21,t}^x & q_{22,t}^x & \cdots & q_{21,t}^x \\ \vdots & \cdots & \ddots & \vdots \\ q_{n1,t}^x & \cdots & \cdots & q_{nn,t}^x \end{pmatrix}. \tag{5}$$

Elements are of the form $q_{ij,t}^x = p_{ij,t}^x s_{ij,t}^x$, which represents the proportion of individuals of class x that move, $p_{ij,t}^x$, and survive, $s_{ij,t}^x$, the transition from node i to node j at time t. Each element is a product of two probabilities and must therefore be a non-negative number less than or equal to 1.

The population projected over an entire annual cycle, beginning at any time t, is given by the seasonal product matrix, $\hat{\mathbf{A}}_t = A_{t+s-1} \cdots A_{t+1} A_t$. The transpose of this product matrix,

$$\hat{\mathbf{A}}_t^T = \prod_{\tau=t}^{t+s-1} \mathbf{A}_\tau^T = A_t^T A_{t+1}^T \cdots A_{t+s-1}^T, \tag{6}$$

will be used to calculate the per-capita contribution metric.

It is important to note two features of our model. First, we have chosen in the formulation of $\mathbf{A}_t$ to apply demographic updates after each dispersal

event. Switching this order would modify $\mathbf{A}_t$ (Hunter and Caswell, 2005). Second, our framework is flexible to handle population models that have density-dependent reproduction, survival, and movement probabilities. For example, if the survival rates of a migration model are seasonal and density-dependent, then $\mathbb{F}_t \equiv \mathbb{F}\left(\vec{\mathbf{N}}_t, t\right)$, $\mathbb{Q}_t \equiv \mathbb{Q}\left(\vec{\mathbf{N}}_t, t\right)$ and $\mathbf{A}_t \equiv \mathbf{A}\left(\vec{\mathbf{N}}_t, t\right)$ will be time- and density-dependent matrices. As such, population abundance at the beginning of the time-step can be determined by solving the following recurrence relation,

$$\vec{\mathbf{N}}_{t+1} = \mathbf{A}_t \vec{\mathbf{N}}_t, \tag{7}$$

where $\vec{\mathbf{N}}_t$ is an $nc \times 1$ block vector whose $c \times 1$ subvectors $\vec{\mathbf{N}}_{i,t}$ give the class distribution within each node i at time t. Furthermore, $\vec{\mathbf{N}}_{t+s} = \hat{\mathbf{A}}_t \vec{\mathbf{N}}_t$ will give the population size after one annual cycle provided $\vec{\mathbf{N}}_t$, and the annual population growth rate for anniversary date t can be defined as $\lambda_t = \vec{\mathbf{w}}_t \hat{\mathbf{A}}_t^T \vec{\mathbf{1}}_{nc}$. Here, $\vec{\mathbf{w}}_t = \vec{\mathbf{N}}_t^T / N_t^{tot}$ is the population proportion at time t, where N_t^{tot} is the network population size (summed across all nodes and all classes during time step t), and $\vec{\mathbf{1}}_{nc}$ is a $nc \times 1$ vector of ones. More details on model construction can be found in the Supplementary Material.

2.1. Habitat Contribution Metric

Wiederholt et al. (2018), following Runge et al. (2006), defined the per-capita contribution, C^r, of a focal habitat r as the expected number of individuals generated from an adult individual occupying the focal habitat in a given year. The value of this metric depends on the anniversary season, which we define as the season from which C^r is calculated. C^r can differ, for example, if it is calculated from spring to spring vs. fall to fall in the same network. The C^r metric is specific for a system of two classes (adults and juveniles), and two seasons so that their formulation only considered two time steps in the annual cycle. This metric assumes juveniles and adults have the same movement transition probabilities. It also assumes juveniles born in the breeding season remain juveniles in the subsequent migratory period. Furthermore, although

the metric accounted for differing survival rates between adults and juveniles, the per-capita contribution metric was only calculated for adults.

We begin by extending C^r in several ways. First, given a focal habitat and anniversary date, we define a per-capita contribution metric C that can be calculated for any class. Our notation of this metric differs from previous works (Runge et al., 2006; Wiederholt et al., 2018) in that the focal node and time-step are given as subscripts and the class is a superscript. For instance, $C^J_{r,t}$ is the number of individuals that are generated after one annual cycle (by time $t+s$), from a single juvenile individual occupying the focal habitat r in the previous year, with anniversary date t. We also generalize the metric for class-specific movement transition probabilities, transitions between ages or stages, and breeding may occur at any time (and possibly multiple times) during the annual cycle. Furthermore, the C-metric can account for any number of seasons and any number of classes or stages.

Formally, $C^x_{r,t}$ is the expected contribution (of a single individual of class x and its offspring) starting at node r and time t to the whole population after one annual cycle. $C^x_{r,t}$ is calculated by summing the contributions from all possible demographic and movement transitions that may happen to an individual moving forward through one annual cycle. We will use matrix algebra to calculate the C-metric for every node, class, and anniversary season.

We define $\vec{\mathbf{C}}_t$ as a block vector whose elements are $C^x_{r,t}$:

$$\vec{\mathbf{C}}_t = \begin{bmatrix} C^1_{1,t} \\ C^2_{1,t} \\ \vdots \\ C^c_{1,t} \\ C^1_{2,t} \\ C^2_{2,t} \\ \vdots \\ C^c_{n,t} \end{bmatrix}$$

The data required to calculate the values of this vector are contained in the

annual projection matrix, defined in eqs. (1) - (6). We solve for $\vec{\mathbf{C}}_t$ by taking the product of the transpose of the annual projection matrix and an $nc \times 1$ vector of ones:

$$\vec{\mathbf{C}}_t = \left(\prod_{\tau=t}^{t+s-1} \mathbf{A}_\tau^T \right) \vec{\mathbf{1}}_{nc} = \hat{\mathbf{A}}_t^T \vec{\mathbf{1}}_{nc}. \tag{8}$$

This matrix product sums across possible annual pathways that migrants can take throughout the annual cycle. If $C_{r,t}^x$ is greater than one, a single individual of class x starting at time t and node r is expected to replace itself and add to the size of the population. If $C_{r,t}^x$ is less than one, individuals do not replace themselves and thus their contribution reduces overall population size. A diagram of how the C-metric is calculated is given in Figure 1.

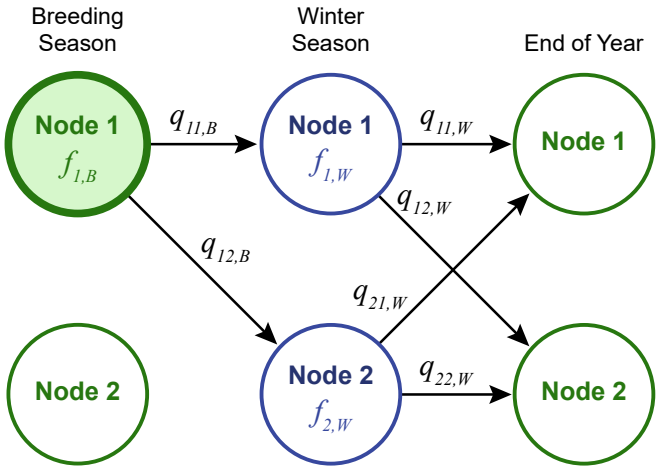

Figure 1: Conceptual diagram of the habitat C-metric. We use the network of a hypothetical metapopulation model with one class. In this illustration, a single individual begins at Node 1 during the breeding season and is tracked over the course of one annual cycle. There are a total of four pathways this individual may take: 111, 112, 121, and 122. The calculation for the per-capita habitat contribution is the sum of contributions of all four possible pathways: $C_{1,B} = f_{1,B}q_{11,B}f_{1,W}q_{11,W} + f_{1,B}q_{11,B}f_{1,W}q_{12,W} + f_{1,B}q_{12,B}f_{2,W}q_{21,W} + f_{1,B}q_{12,B}f_{2,W}q_{22,W}$.

To use the C-metric for assessing the quality of habitats, regardless of class, we must average. We use a class population-weighted average to obtain a single

metric for each habitat and anniversary season,

$$C_{r,t} = \sum_{x=1}^{c} \frac{N_{r,t}^{x}}{N_{r,t}} C_{r,t}^{x}, \tag{9}$$

where $N_{r,t}$ is the population size of node r at time t and $N_{r,t}^{x}/N_{r,t}$ is the proportion of individuals of class x at the node. This results in a single per-capita contribution value for each node r beginning in time step t. This metric indicates whether the focal node is a source ($C_{r,t} > 1$) or a sink ($C_{r,t} < 1$) at time t. Next, since $C_{r,t}$ depends on the anniversary season, to obtain a single node metric, regardless of anniversary season, we use a seasonal population weighted average,

$$\overline{C}_r = \frac{\sum_{\tau=t}^{t+s-1} N_{r,\tau} C_{r,\tau}}{\sum_{\tau=t}^{t+s-1} N_{r,\tau}}. \tag{10}$$

This calculation gives more weight to a season in which the node's population size is large relative to the other seasons.

Similar to the contribution metrics developed by Runge et al. (2006) and Wiederholt et al. (2018), the generalized metric presented here, when weighted by the fraction of the population they represent, sums to the annual population growth rate for each anniversary date, $\lambda_t = \vec{\mathbf{w}}_t \vec{\mathbf{C}}_t$, where $\vec{\mathbf{w}}_t$ is the population proportion.

2.2. Pathway Contribution Metric

We extend the work of Wiederholt et al. (2018) and provide a generalized formulation of the per-capita contribution of edge, or pathway, transitions. The annual per-capita contribution of an individual of class x starting at node r and traveling to node d at time t is

$$C_{rd,t}^{x} = \frac{\vec{\mathbf{1}}_{nc}^{T}}{p_{rd,t}^{x}} \left(\left(\mathbf{A}_t^T \circ (\mathbf{E}_{n,rd} \otimes \mathbf{H}_{c,x}) \right) \prod_{\tau=t+1}^{t+s-1} \mathbf{A}_\tau^T \right) \vec{\mathbf{1}}_{nc}, \tag{11}$$

where $\circ$ is the Hadamard (entrywise) product, $p_{rd,t}^{x}$ is the proportion of individuals of class x at node r that will travel to node d at time t (contained in movement matrix $\mathbf{Q}_t^x$ of eq. (5)), and $\mathbf{H}_{c,x}$ is a $c \times c$ zero matrix with ones in

column x. Recall that $\mathbf{E}_{n,rd}$ is an $n \times n$ zero matrix with a 1 at position rd. If at time t no individuals of class x use edge rd ($p^x_{rd,t} = 0$), then $C^x_{rd,t} = 0$. While the equation for pathway contribution is more cumbersome, the generalized calculation remains straightforward for any number of classes (or stages), a variety of migration strategies, and any number of seasons.

Similar to averaging the metric for habitat contribution given an anniversary season, we construct a single metric for pathway contribution. We weight each $C^x_{rd,t}$ by the number of migrants of class x that use edge rd at time t to obtain

$$C_{rd,t} = \frac{\sum_{x=1}^{c} p^x_{rd,t} N^x_{r,t} C^x_{rd,t}}{\sum_{x=1}^{c} p^x_{rd,t} N^x_{r,t}}. \tag{12}$$

Then by averaging across classes and seasons, we obtain a single metric for each edge,

$$\overline{C}_{rd} = \frac{\sum_{\tau=t}^{t+s-1} \sum_{x=1}^{c} p^x_{rd,t} N^x_{r,\tau} C^x_{rd,\tau}}{\sum_{\tau=t}^{t+s-1} \sum_{x=1}^{c} p^x_{rd,t} N^x_{r,\tau}}. \tag{13}$$

3. Case Studies

In this section, we show that the C-metric can be calculated for populations representing a diverse range of life histories, movement patterns, and carrying capacities. We first apply our model to a simple hypothetical metapopulation to demonstrate matrix construction and illustrate results, and then to three migratory populations: the simpler example of seasonal partial migration of elk, the more complicated seasonal complete migration of northern pintails, and finally the stepping stone migration of monarch butterflies. We note that the parametrization and modeling of these migratory populations have been developed previously (Sample et al., 2018); the results presented in this paper are in the application of the C-metric.

For ease of discussion, in each example we simulate population dynamics until equilibrium, or steady state, is reached; however, the metric does not

require the equilibrium assumption. Variables used in our calculations of the C-metric are determined by their values at the end of these numerical simulations. We assume equilibrium has been reached when the population is within ± 0.01 individuals from one year to the next, comparing like seasons. We note that the C-metric can be calculated using non-equilibrium parameter values that change from one annual cycle to the next. This would lead to network growth rates that are greater or less than one and C-metric values that change from one year to the next. See the Supplemental Information for details of model setup, and Bieri et al. (2019) for parameter values and code developed in R to calculate these metrics for each example.

3.1. Hypothetical Metapopulation

We begin with a simple hypothetical metapopulation model. In this network (Figure 2), there are two nodes, two classes, and two seasons. The two classes are juveniles (J) and adults (A) and the two seasons are breeding (B) and wintering (W). In one time step (one season), individuals can either remain in the same node or disperse to the other node by traveling along weighted and directed edges in the network. In this hypothetical network, node 2 is of lower quality (e.g. lower carrying capacity) compared to node 1.

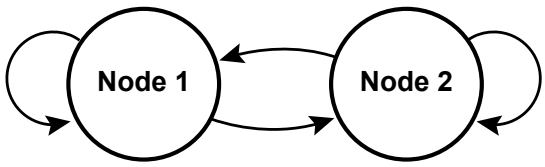

Figure 2: Hypothetical metapopulation network diagram. Both nodes have year-round residents, and both have individuals that move to the other node after breeding and after the winter season.

At the beginning of the breeding season, the population sizes, rounded to the nearest whole number, of juveniles and adults are $N^J_{1,B} = 115$, $N^A_{1,B} = 245$ at node 1, and $N^J_{2,B} = 50$ and $N^A_{2,B} = 105$ at node 2. Juveniles then transition

to adults with some survival probability, adults survive, and surviving adults produce new juveniles. Survival rates are the same across seasons and are given by $s_1^A = 0.9$, $s_1^J = 0.8$, $s_2^A = 0.7$ and $s_2^J = 0.6$. We assume node 1 is closer to its carrying capacity than node 2, and set the reproductive rates as $r_1 = 0.6665$ and $r_2 = 0.5813$. At the end of the breeding season, individuals disperse within the network. The post-breeding, wintering populations are $N_{1,W}^J = 155$, $N_{1,W}^A = 290$, $N_{2,W}^J = 70$ and $N_{2,W}^A = 125$. Individuals survive the winter season with the same probabilities as in the breeding season. In our calculations, we sort by nodes then classes, so that the population vector is given by $\mathbf{N}_t^T = \left[N_{1,t}^J \; N_{1,t}^A \; N_{2,t}^J \; N_{2,t}^A\right]^T$.

To formulate $\mathbf{A}_t$, we begin by constructing matrices $\mathbb{F}_t$ and $\mathbb{Q}_t$. We create these matrices for the breeding ($t = B$) and wintering ($t = W$) seasons at steady state. During the breeding season, the demographic matrix of eq. (3) is

$$\mathbf{F}_{i,B} = \begin{bmatrix} 0 & s_i^J \\ r_i & s_i^A \end{bmatrix}, \quad i = 1, 2.$$

Here, the elements in the top row represent juvenile survival and juvenile transition to adults, respectively. Note that all surviving juveniles transition to adults in this season. The bottom row represents reproduction (adults creating juveniles) and adult survival, respectively. During the wintering season, there are no class transitions and only survival within the classes:

$$\mathbf{F}_{i,W} = \begin{bmatrix} s_i^J & 0 \\ 0 & s_i^A \end{bmatrix}, \quad i = 1, 2.$$

The demographic block matrices of eq. (2) for the breeding and wintering seasons

are

$$\mathbb{F}_B = \left(\begin{array}{c|c} \mathbf{F}_{1,B}^T & 0 \\ \hline 0 & \mathbf{F}_{2,B}^T \end{array}\right) = \begin{pmatrix} 0 & 0.6665 & 0 & 0 \\ 0.8 & 0.9 & 0 & 0 \\ 0 & 0 & 0 & 0.5813 \\ 0 & 0 & 0.6 & 0.7 \end{pmatrix}$$

$$\mathbb{F}_W = \left(\begin{array}{c|c} \mathbf{F}_{1,W}^T & 0 \\ \hline 0 & \mathbf{F}_{2,W}^T \end{array}\right) = \begin{pmatrix} 0.8 & 0 & 0 & 0 \\ 0 & 0.9 & 0 & 0 \\ 0 & 0 & 0.6 & 0 \\ 0 & 0 & 0 & 0.7 \end{pmatrix}$$

We now set up the matrices of eq. (5). In this hypothetical model, movement does not depend on class or season and individuals are more likely to remain residents than disperse to the other node. Individuals have an 80% probability of remaining at node 1 and a 60% probability of remaining at node 2. Therefore, the matrices of eq. (5), which are class- and time-independent in this model, are

$$\mathbf{Q}^J = \mathbf{Q}^A = \begin{bmatrix} 0.8 & 0.2 \\ 0.4 & 0.6 \end{bmatrix}$$

Thus, the movement block matrices of eq. (4) are

$$\mathbb{Q}_B = \mathbb{Q}_W = (\mathbf{Q}^J)^T \otimes \begin{bmatrix} 1 & 0 \\ 0 & 0 \end{bmatrix} + (\mathbf{Q}^A)^T \otimes \begin{bmatrix} 0 & 0 \\ 0 & 1 \end{bmatrix}$$

$$= \begin{bmatrix} 0.8 & 0 & 0.4 & 0 \\ 0 & 0.8 & 0 & 0.4 \\ 0.2 & 0 & 0.6 & 0 \\ 0 & 0.2 & 0 & 0.6 \end{bmatrix}$$

From eq. (1), we have the following projection matrices for the breeding and

wintering seasons,

$$\mathbf{A}_B = \mathbb{Q}_B\mathbb{F}_B = \begin{bmatrix} 0 & 0.5332 & 0 & 0.2325 \\ 0.6400 & 0.7200 & 0.2400 & 0.2800 \\ 0 & 0.1333 & 0 & 0.3488 \\ 0.1600 & 0.1800 & 0.3600 & 0.4200 \end{bmatrix}$$

$$\mathbf{A}_W = \mathbb{Q}_W\mathbb{F}_W = \begin{bmatrix} 0.6400 & 0 & 0.2400 & 0 \\ 0 & 0.7200 & 0 & 0.2800 \\ 0.1600 & 0 & 0.3600 & 0 \\ 0 & 0.1800 & 0 & 0.4200 \end{bmatrix}$$

We calculated the per-capita contributions for each node, class and anniversary season using the matrix multiplication defined in eq. (8). At equilibrium, the per-capita contribution equations for the breeding and wintering seasons are

$$\vec{\mathbf{C}}_B = \mathbf{A}_B^T\mathbf{A}_W^T\vec{\mathbf{1}}_4,$$
$$\vec{\mathbf{C}}_W = \mathbf{A}_W^T\mathbf{A}_B^T\vec{\mathbf{1}}_4.$$

We then use eq. (9) to average across classes and eq. (10) to average across seasons. Adults, who contribute to the population through reproduction, have higher C-values than juveniles (Table 4). After averaging across classes, our results indicate that an individual at node 1 is expected to contribute more individuals to the network than an individual from node 2. We categorize node 1 as a source ($C_r > 1$) and node 2 as a sink ($C_r < 1$).

The pathway that represents node 1's resident population (C_{11}) has a higher contribution value and the pathway representing node 2's resident population (C_{22}) has a lower value (Table 5).

Metapopulation Model				
Node		Breeding Season	Winter Season	Seasonal Average
Node 1 juveniles	$C_{1,t}^{J}$	0.6880	0.6080	-
Node 1 adults	$C_{1,t}^{A}$	1.2805	1.3585	-
Node 2 juveniles	$C_{2,t}^{J}$	0.4680	0.4080	-
Node 2 adults	$C_{2,t}^{A}$	0.9413	0.9768	-
Node 1 (class avg)	$C_{1,t}$	1.0903	1.0981	1.0946
Node 2 (class avg)	$C_{2,t}$	0.7890	0.7736	0.7804

Table 4: Per-capita contribution of each node for the hypothetical metapopulation example.

Metapopulation Model				
Pathway		Breeding Season	Winter Season	Seasonal Average
Edge 1→1 juveniles	$C_{11,t}^{J}$	0.5332	0.6400	-
Edge 1→1 adults	$C_{11,t}^{A}$	1.5300	1.4099	-
Edge 1→2 juveniles	$C_{12,t}^{J}$	0.3999	0.4800	-
Edge 1→2 adults	$C_{12,t}^{A}$	1.1900	1.1532	-
Edge 2→1 juveniles	$C_{21,t}^{J}$	0.4650	0.4800	-
Edge 2→1 adults	$C_{21,t}^{A}$	1.1700	1.0965	-
Edge 2→2 juveniles	$C_{22,t}^{J}$	0.3488	0.3600	-
Edge 2→2 adults	$C_{22,t}^{A}$	0.9100	0.8969	-
Edge 1→1 (class avg)	$C_{11,t}$	1.2100	1.1428	1.1728
Edge 1→2 (class avg)	$C_{12,t}$	0.9364	0.9196	0.9271
Edge 2→1 (class avg)	$C_{21,t}$	0.9432	0.8763	0.9060
Edge 2→2 (class avg)	$C_{22,t}$	0.7294	0.7051	0.7159

Table 5: Per-capita contribution of each pathway for the hypothetical metapopulation example.

3.2. Elk in the Greater Yellowstone Ecosystem

We apply our model of habitat and pathway contribution to a population of elk located in the Greater Yellowstone Ecosystem (henceforth, Yellowstone). To parameterize the model, we begin with the modeling framework presented in Sample et al. (2018), with model parameters and density-dependent assumptions based on the literature (Singer et al., 1997; Taper and Gogan, 2002; Middleton et al., 2013). Values of the parameters at equilibrium were used to calculate the C-metric.

Elk partially migrate among three geographical locations (Figure 3). One location (Node 3) is near Cody, Wyoming, where two groups of elk reside, one that remains resident year-round and another that migrates to Yellowstone. The elk that remain resident year-round in Node 3 breed there in the summer season. Yellowstone (Node 1) is the summering location where migrating elk breed, and the location between Cody and Yellowstone (Node 2) is where migrating elk winter. All elk in this location migrate to Yellowstone during the summer for breeding (Middleton et al., 2013). One annual cycle comprises two seasons. Season 1 includes winter and spring migration, and Season 2 includes summer and fall migration. We modeled female elk of two classes, juveniles (J) and adults (A). During Season 1, juveniles and adults survive at class specific survival rates. During Season 2, all surviving juveniles transition into adults, surviving adults reproduce and create juveniles, and adults survive.

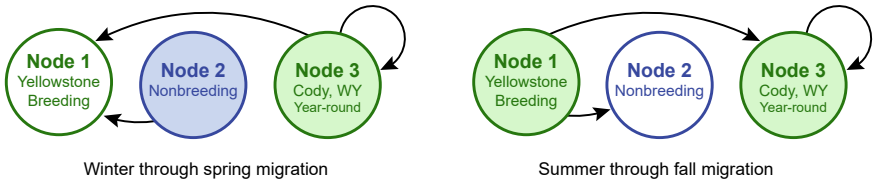

Figure 3: Network model for elk in the Greater Yellowstone Ecosystem. Nodes that are occupied at the start of the focal time interval are shaded.

We obtained the per-capita contributions for each class at each node and average across classes and seasons at equilibrium according to eqs. (9) and (10).

The average per-capita contributions were close to 1 for every node (Table 6). Node 2 had a slightly higher per-capita contribution than the other nodes. This indicates that an individual starting in the wintering node is expected, on average, to contribute more individuals to the population compared to the breeding and year-round nodes. However, as the per-capita contributions were near 1 ($C_r < 0.8\%$ within 1), none of the nodes could be clearly classified as a source or sink.

Results for the pathway metric, presented in Table 7, demonstrate that the fall migration paths (from Node 1 to Node 2 and from Node 1 to Node 3) have the largest per-capita contribution. The other three edges have per-capita contributions close to 1, with the spring migration route from Node 3 to Node 1 as the only path considered a sink.

Elk Model				
Node		Winter/ Spring	Summer/ Fall	Seasonal Average
Node 1 (Breeding)	$C_{1,t}$	0	1.0000	1.0000
Node 2 (Nonbreeding)	$C_{2,t}$	1.0072	0	1.0072
Node 3 (Year-round)	$C_{3,t}$	0.9961	1.0000	0.9978

Table 6: Per-capita contribution of each node for the elk example. The metric $C_{r,t}$ equals zero when no individuals reside in node r during time step t.

Elk Model				
Pathway		Winter/ Spring	Summer/ Fall	Seasonal Average
Fall Edge 1→2	$C_{12,t}$	0	1.2205	1.2205
Fall Edge 1→3	$C_{13,t}$	0	1.1475	1.1475
Spring Edge 2→1	$C_{21,t}$	1.0072	0	1.0072
Spring Edge 3→1	$C_{31,t}$	0.9522	0	0.9522
Resident Edge 3→3	$C_{33,t}$	1.0000	1.1310	1.0580

Table 7: Per-capita contribution of each pathway for the elk example.

3.3. Northern Pintail

Northern pintail is widely distributed in wetland regions; it breeds in the northern areas of North America, Europe, and Asia and winters from southern temperate to tropical regions of the northern hemisphere (BirdLife International, 2019). The population model in Sample et al. (2018), which used the parameter values and model assumptions from Mattsson et al. (2012), has four classes, three seasons and five nodes. The four population classes are adult males (AM), adult females (AF), juvenile males (JM), and juvenile females (JF). The annual cycle is divided into three seasons: breeding, wintering and spring flyover. Nodes 1 through 3 (i.e., Alaska (AK), Prairie Potholes (PR) and Northwest Unsurveyed (NU)), are breeding habitats whereas Nodes 4 and 5 (i.e., California (CA) and Gulf Coast (GC)), are wintering habitats (Figure 4). In the wintering Season 2, all juveniles transition to adults. No births, deaths or age transitions occur during the flyover Season 3; rather, migrants decide whether to stay in PR or continue (flyover) to AK or NU. In the model, proportion of flyovers is density-dependent and evaluated at population equilibrium.

We calculate the per-capita contributions averaged across classes and seasons at equilibrium (Table 8). On average, a single individual starting in nodes 2 (PR) or 5 (GC) is expected to contribute more individuals to the population than it loses, whereas the opposite is true for an individual starting at nodes 1 (AK), 3 (NU) and 4 (CA). As such, PR and GC are sources and the remaining habitats are sinks.

The spring migratory paths from the wintering nodes (CA and GC) had the largest contribution (Table 9). The fall migratory pathways from the breeding nodes (AK, PR, and NU) to the wintering nodes (CA and GC) had the smallest contributions.

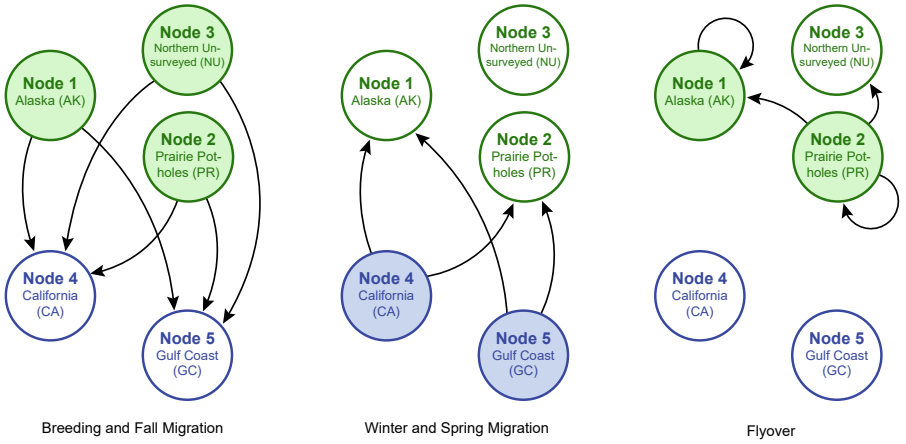

Figure 4: Network model for the northern pintail. Nodes that are occupied at the start of the focal season are shaded.

Pintail Model					
Node		Breeding/ Fall	Winter/ Spring	Flyover	Seasonal Average
Node 1 (AK)	$C_{1,t}$	0.9916	0	0.9917	0.9917
Node 2 (PR)	$C_{2,t}$	1.1347	0	1.0053	1.0479
Node 3 (NU)	$C_{3,t}$	0.8684	0	0	0.8684
Node 4 (CA)	$C_{4,t}$	0	0.9759	0	0.9759
Node 5 (GC)	$C_{5,t}$	0	1.0493	0	1.0493

Table 8: Per-capita contribution of each node in the pintail migratory network. The metric $C_{r,t}$ equals zero when no individuals reside in node r during time step t.

Pintail Model		
Pathway		Seasonal Average
Fall AK→CA	$C_{14,t}$	0.6958
Fall AK→GC	$C_{15,t}$	0.7127
Fall PR→CA	$C_{24,t}$	0.6958
Fall PR→GC	$C_{25,t}$	0.7547
Fall NU→CA	$C_{34,t}$	0.6958
Fall NU→GC	$C_{35,t}$	0.7547
Spring CA→AK	$C_{41,t}$	1.3593
Spring CA→PR	$C_{42,t}$	1.3381
Spring GC→AK	$C_{51,t}$	1.4911
Spring GC→PR	$C_{52,t}$	1.4678
Flyover AK→AK	$C_{11,t}$	0.9917
Flyover PR→AK	$C_{21,t}$	0.9913
Flyover PR→PR	$C_{22,t}$	1.1347
Flyover PR→NU	$C_{23,t}$	0.8684

Table 9: Per-capita contribution of each pathway in the pintail migratory network. Each pathway is used only once during the annual cycle, so each seasonal average is equal to the one non-zero value of the metric.

3.4. Monarch Butterfly

Monarch butterfly in eastern North America migrate from breeding areas in the northern U.S. and southern Canada to a non-breeding area in central Mexico. The population model developed in Flockhart et al. (2015) was converted to a network-based model using the framework presented in Sample et al. (2018). There is one class (adult females), seven seasons and four nodes. The seven seasons of the annual cycle are: Winter (October through May), April, May, June, July, August, and September. Breeding occurs April through September. The four nodes represent regions of eastern North America: Mexico (M), South (S), Central (C), and North (N), enumerated 1 through 4, respectively (Figure 5). Mexico is considered a wintering node and the other three nodes are breeding nodes. Seasonal edge transition and survival probabilities are assumed to be constant from year to year.

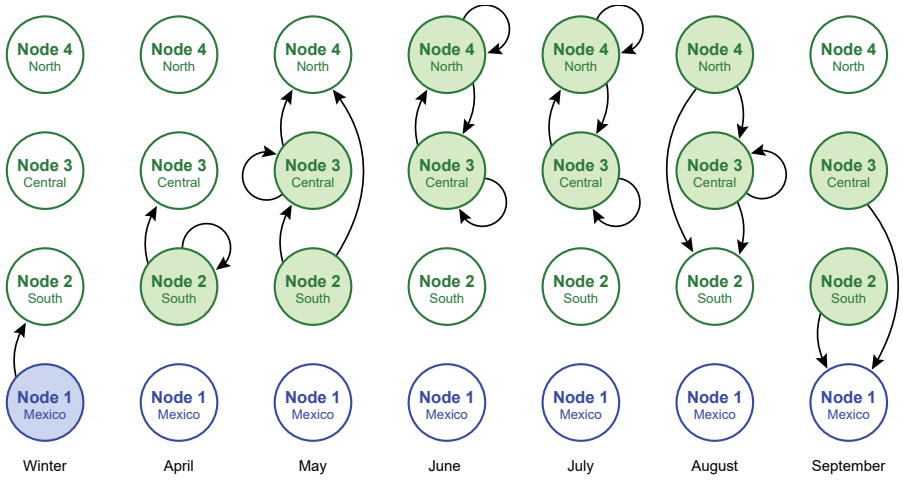

Figure 5: Monarch network model. Nodes that are occupied at the start of the focal season are shaded.

Based on the C-metric, an individual starting in the North (Node 4) is expected to contribute the least to the population, whereas an individual starting in the Central region (Node 3) is expected to contribute the most (Table 10). Note that all individuals reside in Mexico (Node 1) and the South (Node 2)

during Winter and April, respectively. Therefore, the per-capita contributions of Mexico and South are equivalent to the network growth rate ($\lambda = 1$) during these seasons. This is true even when the network is out of equilibrium. Thus, given a C-metric of 1, each individual wintering in Mexico or residing in the South in April, is expected to replace itself over the annual cycle. Considering the per-capita contributions of the pathways, the resident transition in the Central node contributes the most whereas the spring migration from South to North contributes the least (Table 11).

Monarch Model									
Node		Winter	April	May	June	July	August	Sept.	Avg.
Mexico (M)	$C_{1,t}$	1.0000	0	0	0	0	0	0	1.0000
South (S)	$C_{2,t}$	0	1.0000	0.7715	0	0	0	1.0177	0.9415
Central (C)	$C_{3,t}$	0	0	1.5084	1.0636	1.7442	1.2344	0.9834	1.2468
North (N)	$C_{4,t}$	0	0	0	0.8974	0.6139	0.7582	0	0.7157

Table 10: Per-capita contribution of each node for the monarch example. Since there is only one class, $C^x_{r,t} = C_{r,t}$. Note that the metric equals zero when no individuals reside in node r during time step t.

Monarch Model									
Node		Winter	April	May	June	July	August	Sept.	Avg.
Edge $M \to S$	$C_{12,t}$	1.0000	0	0	0	0	0	0	1.0000
Edge $S \to M$	$C_{21,t}$	0	0	0	0	0	0	1.0177	1.0177
Edge $S \to S$	$C_{22,t}$	0	0.8588	0	0	0	0	0	0.8587
Edge $S \to C$	$C_{23,t}$	0	1.2305	0.9251	0	0	0	0	1.0573
Edge $S \to N$	$C_{24,t}$	0	0	0.5793	0	0	0	0	0.5793
Edge $C \to M$	$C_{31,t}$	0	0	0	0	0	0	0.9834	0.9833
Edge $C \to S$	$C_{32,t}$	0	0	0	0	0	1.0798	0	1.0798
Edge $C \to C$	$C_{33,t}$	0	0	1.8284	1.8468	2.0845	1.4233	0	1.7825
Edge $C \to N$	$C_{34,t}$	0	0	1.1447	0.4823	0.9501	0	0	0.7185
Edge $N \to S$	$C_{42,t}$	0	0	0	0	0	0.6689	0	0.6689
Edge $N \to C$	$C_{43,t}$	0	0	0	1.5729	0.7011	0.8816	0	0.8775
Edge $N \to N$	$C_{44,t}$	0	0	0	0.7461	0.5804	0	0	0.6297

Table 11: Per-capita contribution of each pathway in the monarch migratory network. M, S, C, and N indicates nodes Mexico, South, Central, and North, respectively.

4. Discussion

We have shown how the demographic contributions of individuals from discrete habitats can be quantified by a generalized C-metric and that this generalization can describe populations exhibiting a diversity of movement strategies. The metric can be applied to a wide range of spatially structured populations with any number of classes, seasons, or types of movement strategies including simple two-patch systems, complex metapopulations, and complete seasonal migration. This metric is simple to calculate as long as estimates for seasonal demographic and movement parameters are available. It does not require density-dependent functions, although these can be incorporated in the projection matrix. It also does not require the population to be at equilibrium. While the metric is sufficiently general to be applied to metapopulation networks, as in the simple example we provided and as shown in more complex examples (e.g., Strasser et al.,2012), we found it particularly useful for gaining a better understanding about the roles of discrete habitats in migratory networks.

In the elk example, Middleton et al. (2013) found that elk migrating each spring into Yellowstone National Park had declining calf recruitment and pregnancy rates. This process was captured through the low pathway contribution value for the Spring edge from 3 to 1 and with the overall lower node contribution value for Node 3. These findings indicate that the Year-Round Cody WY area was potentially a minor sink subpopulation in 2009, given the C_r values slightly below 1, and that the role of this region in the overall population has shifted as habitat quality declined from 1989 to 2009.

Results from the pintail example matched some expectations but not others. The Prairie Pothole region (PR) is recognized as providing crucial breeding habitat for many migratory waterfowl species, including the pintail (Podruzny et al., 2002; Doherty et al., 2016). PR had the highest C_r value among regions and serves as a strong source ($C_r \geq 5\%$ above 1), in alignment with expectations. The role of wintering areas has until now been viewed as secondary (Miller et al., 2003), but we found that at equilibrium an individual overwintering in

the Gulf Coast habitat contributed nearly the same number of individuals to the population as did an individual that bred in the PR. This contradicts findings of a perturbation analysis, which showed that increasing reproduction in the PR by 10% had a larger effect on continental-scale carrying capacity than did increasing habitat area by 10% in the Gulf Coast habitat (Mattsson et al., 2012). There was a disparity between the two wintering regions in terms of their per-capita contributions, which we did not expect. Although the habitat in California supports more overwintering individuals at carrying capacity, it acts like a weak sink (C_r is $\leq$5% below 1) due to most California birds migrating to Alaska where reproduction is insufficient to maintain a growing population on its own. We also found that the Northern Unsurveyed habitat serves as a strong sink (C_r is >5% below 1). This is in line with our expectation that this habitat plays a minor role in continental population dynamics due to having substantially lower reproduction compared to the other breeding habitats. The Northern Unsurveyed habitat serves as a spillover habitat when the population nears carrying capacity in the PR. Comparing C_r values among core breeding and wintering habitats used by pintails provides additional insight and perspectives on the relative importance of these habitats to the population at a continental scale.

In the monarch case study, we found that the Central region had the highest seasonally averaged C_r, and the North had the lowest. This qualitative prioritization of the Central region matches the sensitivity analyses done by Flockhart et al. (2015) and Oberhauser et al. (2017). Flockhart et al. (2015) performed an elasticity analysis of demographic and migration parameters in their matrix model and summed these elasticities across geographic regions to compare regional contributions to population size. Their analyses showed the Central region had the highest summed elasticity, followed by the South, then Mexico, then the North. C_r ranked Mexico slightly higher than the South while elasticities were higher for the South than Mexico. An important area of future work would include a more thorough analysis of, and comparison between, results from elasticity analysis and more direct metrics like the C-metric. Fur-

thermore, it would be interesting to extend the elasticity analysis of population abundance (Flockhart et al., 2015) by examining the sensitivity of C_r to uncertainties in the demographic parameters.

The C-metric for edges describes how individuals traveling along an edge contribute to the population. Insight about the source or sink value of the edge can be gained when comparing edges within the same season. For example, in the elk model, individuals traveling along the edge between the breeding and nonbreeding nodes during fall migration contribute more to the population than are lost, meaning that the pathway is a source. Individuals choosing to migrate from Cody (year-round node) to Yellowstone (breeding node) in the spring contribute less to the population than individuals choosing to remain in Cody or to migrate along a shorter path. Considering the pintail pathway rankings, spring migration pathways act as sources whereas fall migration pathways serve as sinks. We see similar results with monarchs—pathways with strong connections with the Central node (a strong source) have higher C_{rd} values, meaning that individuals flowing along these paths contribute more to the population than are lost due to mortality. In general, the pathway metric for fall edges are larger than for spring edges. This can be accounted for by the census date.

Census dates are an important part of understanding C-metric values. When calculating C_r at the nodes, the census is taken at the beginning of the season, which is before reproduction and habitat survival occurs. For the pathway metric, the census is taken after reproduction and habitat survival occurs (right before individuals move along the pathway). Thus, direct comparison between node and edge values is complicated because of this difference in census date. This discordance means that C-metric values are highly dependent on both the census date and the focal season and more work is needed to understand the consequence of these differences on implications for management.

The per-capita contribution metric is useful for identifying source and sink nodes or pathways (Erickson et al., 2018) and for providing information about the reproductive potential of an individual at the node or pathway. However, the C-metric has limitations: it does not include information about network

structure. For example, a node could be rather unimportant in terms of its demographic contribution (sink) yet vital to the connectivity of the network. Given the complexity of spatially structured populations and the numerous ways by which existence or quality of a node or edge can influence the population as a whole, developing a single metric that indicates all dimensions of importance for population dynamics remains elusive. Using multiple metrics is, therefore, a more reliable way of assessing quality of nodes and pathways in a spatially structured population. Furthermore, the calculation of per-capita contribution metrics requires demographic data (survival rates, transition rates between nodes, and reproductive rates) and relative distribution of the population among its constituent habitats. It can be challenging to parameterize models with existing monitoring programs that provide access to data, such as eBird (Sullivan et al., 2009), movebank (Wikelski and Kays, 2019) and Monitoring Avian Productivity and Survival (DeSante et al., 2015). Reverse-time multi-state capture-recapture models can be used in combination with per-capita metrics to estimate the demographic importance of local populations to metapopulation growth (Sanderlin et al., 2011). But if limited or no demographic data are available, then graph-based metrics may be more appropriate (Nicol et al., 2016; Bieri et al., 2018).

To accommodate the full range of life histories expressed by spatially structured populations, contribution metrics should account for different age and stage classes and the anniversary season. Thus, the number of per-capita contribution metrics to compute for a given population amounts to the product of the number of habitats, classes, and seasons. This may be too much information for managers who wish to have one metric per habitat when assessing habitat importance. For this reason, we presented a population-weighted average of the per-capita contributions across classes and seasons for a given habitat or patch. We caution that this may hide ecologically important disparities, and the component metrics should be made available in addition to the weighted averages.

Although it is not required by the formulation, the examples in this paper

assume equilibrium in calculating the C-metric. As such, these examples do not represent populations that are increasing or decreasing. Assuming equilibrium is unrealistic for populations undergoing long-term increases or decreases in abundance. Equilibrium assumptions are, however, commonly used in population ecology, such as the assumption of a stable age distribution in eigen-analyses of Leslie/Lefkovitch matrices (Caswell, 2001). As of yet, it is not well understood how equilibrium assumptions might affect the ranking of importance of habitats as indicated by the C-metric. That is, the habitat with the highest per-capita contribution at equilibrium could be superseded by another habitat when the population is growing or declining. This question is worthy of future exploration. As in spatially unstructured models (Gamelon et al., 2014), we anticipate that the study of transient dynamics in spatially structured populations could lead to a rich body of knowledge about how per-capita contributions shift in response to natural disturbance or management actions, and how these effects percolate through a network.

A future extension of the generalized C-metric would allow for estimating the per-capita contribution along a series of pathways (Erickson et al., 2018; Wiederholt et al., 2018) rather than restricting the metric to single interseasonal transitions. For example, waterfowl biologists and managers might be interested in comparing contributions among flyways that encompass habitats used during spring and fall along a migratory route (Kirby et al., 2008; Convention on Migratory Species, 2017). Considering the pintail case, we could then compare the per-capita contribution of birds using the Pacific Flyway to those using the Central Flyway of North America (Buhnerkempe et al., 2016). Under environmental change, we may see shifts in the proportion of the population using these pathways that would also affect per-capita contributions among flyways.

Another important area of future work includes the utility and robustness of the C-metric. Comparing the C-metric to other approaches that rank importance of habitats, like parameter perturbation and simulation, might give a better idea of the true management utility of the C-metric. Also, testing

the sensitivity of the C-metric to changes in network or parameter assumptions would give managers a better idea of error tolerance in, and robustness of, the C-metric ranking.

Generalizing the C-metric opens up diverse research questions. How does per-capita contribution vary among life history strategies, and can this be used to understand the evolution of particular movement strategies such as migration and nomadism? Is C_r a good indicator of the effects of perturbing a habitat or path in a migratory network? Are there ways of using citizen science observations (e.g., from eBird) to estimate C_r? Our generalized modeling framework and computer code will enable population ecologists to pursue these avenues, which will lead to a richer understanding of spatially structured populations. Furthermore, the C-metric, as an estimate of per capita contributions, is an indicator of individual fitness in an area, and may be useful to researchers studying eco-evolutionary dynamics in fragmented landscapes (Legrand et al., 2017), studies of niches in spatial and temporally varying environments (Holt, 2009), and the evolution of dispersal (Cote et al., 2017).

5. Acknowledgments

Funding: This work was supported by the Habitat for Migratory Species Working Group at the National Institute for Mathematics and Biological Synthesis, sponsored by the National Science Foundation (DBI-1300426) and the National Science Foundation RUI Award (DMS-1715315). Additional support from Ecosystems and Land Change Science Programs at the U.S. Geological Survey and the University of Redlands and Emmanuel College summer research programs.

Behrens, V., F. Rauschmayer, and H. Wittmer (2008). Managing international 'problem' species: Why pan-European cormorant management is so difficult. *Environmental Conservation 35*(1), 55–63.

Bieri, J., C. Sample, J. Earl, S. Nicol, W. Thogmartin, R. Erickson, D. Semmens, P. Federico, T. Skraber, J. Diffendorfer, D. Flockhart, R. Wiederholt,

and B. Mattsson (2018). A guide to calculating habitat-quality metrics to inform conservation of highly mobile species. *Natural Resource Modeling 31*(1), e12156.

Bieri, J., C. Sample, S. Stafford, and J. Macias (2019, January). Nimbios-habitatqualitymetrics/generalizedcr (version v1.0.1).

BirdLife International (2019). Species factsheet: *Anas acuta*. `https://www.birdlife.org/` downloaded on 11 Jan 2019.

Buhnerkempe, M. G., C. T. Webb, A. A. Merton, J. E. Buhnerkempe, G. H. Givens, R. S. Miller, and J. A. Hoeting (2016). Identification of migratory bird flyways in North America using community detection on biological networks. *Ecological Applications 26*(3), 740–751.

Caswell, H. (2001). *Matrix Population Models: Construction, Analysis, and Interpretation* (2 ed.). Sunderland: Sinauer Associates.

Convention on Migratory Species (2017). Flyways. `https://www.cms.int/sites/default/files/document/cms_cop12_res.12.11_flyways_e.pdf`.

Cote, J., E. Bestion, S. Jacob, J. Travis, D. Legrand, and M. Baguette (2017). Evolution of dispersal strategies and dispersal syndromes in fragmented landscapes. *Ecography 40*(1), 56–73.

DeSante, D., D. Kaschube, and J. Saracco (2015). Vital rates of North American landbirds. The Institute for Bird Populations.

Doherty, K. E., D. W. Howerter, J. H. Devries, and J. Walker (2016). Prairie pothole region of North America. *The Wetland Book: II: Distribution, Description and Conservation*, 1–10.

Erickson, R. A., J. E. Diffendorfer, D. R. Norris, J. A. Bieri, J. E. Earl, P. Federico, J. M. Fryxell, K. R. Long, B. J. Mattsson, C. Sample, et al. (2018). Defining and classifying migratory habitats as sources and sinks: The migratory pathway approach. *Journal of Applied Ecology 55*(1), 108–117.

Flockhart, D. T. T., J. B. Pichancourt, D. R. Norris, and T. G. Martin (2015). Unravelling the annual cycle in a migratory animal: breeding-season habitat loss drives population declines of monarch butterflies. *Journal of Animal Ecology 84*, 155–165.

Gamelon, M., O. Gimenez, E. Baubet, T. Coulson, S. Tuljapurkar, and J.-M. Gaillard (2014). Influence of life-history tactics on transient dynamics: a comparative analysis across mammalian populations. *The American Naturalist 184*(5), 673–683.

Holt, R. D. (2009). Bringing the Hutchinsonian niche into the 21st century: Ecological and evolutionary perspectives. *Proceedings of the National Academy of Sciences 106*(Supplement 2), 19659–19665.

Hunter, C. and H. Caswell (2005). The use of the vec-permutation matrix in spatial matrix population models. *Ecological Modelling 188*, 15–21.

Johnson, D. W., M. R. Christie, T. J. Pusack, C. D. Stallings, and M. A. Hixon (2018). Integrating larval connectivity with local demography reveals regional dynamics of a marine metapopulation. *Ecology 99*(6), 1419–1429.

Kirby, J. S., A. J. Stattersfield, S. H. Butchart, M. I. Evans, R. F. Grimmett, V. R. Jones, J. O'Sullivan, G. M. Tucker, and I. Newton (2008). Key conservation issues for migratory land-and waterbird species on the world's major flyways. *Bird Conservation International 18*(S1), S49–S73.

Kölzsch, A. and B. Blasius (2008). Theoretical approaches to bird migration. *The European Physical Journal Special Topics 157*(1), 191–208.

Legrand, D., J. Cote, E. A. Fronhofer, R. D. Holt, O. Ronce, N. Schtickzelle, J. M. Travis, and J. Clobert (2017). Eco-evolutionary dynamics in fragmented landscapes. *Ecography 40*(1), 9–25.

Martin, T. G., I. Chads, P. Arcese, P. P. Marra, H. P. Possingham, and D. R. Norris (2007). Optimal conservation of migratory species. *PLoS ONE 2*, e751.

Mattsson, B. J., M. C. Runge, J. H. Devries, G. S. Boomer, J. M. Eadie, D. A. Haukos, J. P. Fleskes, D. N. Koons, W. E. Thogmartin, and R. G. Clark (2012). A modeling framework for integrated harvest and habitat management of North American waterfowl: Case-study of northern pintail metapopulation dynamics. *Ecological Modelling 225*, 146–158.

Middleton, A. D., M. J. Kauffman, D. E. McWhirter, J. G. Cook, R. C. Cook, A. A. Nelson, M. D. Jimenez, and R. Klaver (2013). Animal migration amid shifting patterns of phenology and predation: Lessons from a Yellowstone elk herd. *Ecology 94*(6), 1245–1256.

Miller, M. R., D. C. Duncan, K. Guyn, P. Flint, and J. Austin (2003). The northern pintail in North America: The problem and prescription for recovery. In *Northern Pintail Workshop, 23-25 March 2001.*

Nicol, S., R. Wiederholt, J. Diffendorfer, B. J. Mattsson, W. E. Thogmartin, D. J. Semmens, L. López-Hoffman, and D. R. Norris (2016). A management-oriented framework for selecting metrics used to assess habitat- and path-specific quality in spatially structured populations. *Ecological Indicators 69*, 792–802.

Oberhauser, K., R. Wiederholt, J. Diffendorfer, D. Semmens, L. Ries, W. E. Thogmartin, L. Lopez-Hoffman, and B. Semmens. (2017). A trans-national monarch butterfly population model and implications for regional conservation priorities. *Ecological Entomology 42*, 51–60.

Pascarella, J. B. and C. C. Horvitz (1998). Hurricane disturbance and the population dynamics of a tropical understory shrub: Megamatrix elasticity analysis. *Ecology 79*(2), 547–563.

Podruzny, K. M., J. H. Devries, L. M. Armstrong, and J. J. Rotella (2002). Long-term response of northern pintails to changes in wetlands and agriculture in the Canadian Prairie Pothole region. *The Journal of Wildlife Management*, 993–1010.

Robertson, E. P., R. J. Fletcher, C. E. Cattau, B. J. Udell, B. E. Reichert, J. D. Austin, and D. Valle (2018). Isolating the roles of movement and reproduction on effective connectivity alters conservation priorities for an endangered bird. *Proceedings of the National Academy of Sciences 115*(34), 8591–8596.

Rogers, A. (1966). The multiregional matrix growth operator and the stable interregional age structure. *Demography 3*(2), 537–544.

Runge, C. A., E. Gallo-Cajiao, M. J. Carey, S. T. Garnett, R. A. Fuller, and P. C. McCormack (2017). Coordinating domestic legislation and international agreements to conserve migratory species: A case study from Australia. *Conservation Letters 10*(6), 765–772.

Runge, J., M. Runge, and J. Nichols (2006). The role of local populations within a landscape context: Defining and classifying sources and sinks. *The American Naturalist 167*, 925–938.

Sample, C., J. M. Fryxell, J. A. Bieri, P. Federico, J. E. Earl, R. Wiederholt, B. J. Mattsson, D. T. Flockhart, S. Nicol, J. E. Diffendorfer, et al. (2018). A general modeling framework for describing spatially structured population dynamics. *Ecology and Evolution 8*(1), 493–508.

Sanderlin, J. S., P. M. Waser, J. E. Hines, and J. D. Nichols (2011). On valuing patches: Estimating contributions to metapopulation growth with reverse-time capture–recapture modelling. *Proceedings of the Royal Society B: Biological Sciences 279*(1728), 480–488.

Sawyer, H. and M. J. Kauffman (2011). Stopover ecology of a migratory ungulate. *Journal of Animal Ecology 80*(5), 1078–1087.

Semmens, D., J. Diffendorfer, L. López-Hoffman, and C. Shapiro (2011). Accounting for the ecosystem services of migratory species: Quantifying migration support and spatial subsidies. *Ecological Economics 70*, 2236–2242.

Semmens, D. J., J. E. Diffendorfer, K. J. Bagstad, R. Wiederholt, K. Oberhauser, L. Ries, B. X. Semmens, J. Goldstein, J. Loomis, W. E. Thogmartin,

et al. (2018). Quantifying ecosystem service flows at multiple scales across the range of a long-distance migratory species. *Ecosystem Services 31, Part B*, 255–264.

Singer, F. J., A. Harting, K. K. Symonds, and M. B. Coughenour (1997). Density dependence, compensation, and environmental effects on elk calf mortality in Yellowstone National Park. *Journal of Wildlife Management 61*, 12–25.

Strasser, C., M. Neubert, H. Caswell, and C. Hunter (2012). Contributions of high- and low-quality patches to a metapopulation with stochastic disturbance. *Theoretical Ecology 5*, 167–179. doi:10.1007/s12080-010-0106-9.

Sullivan, B. L., C. L. Wood, M. J. Iliff, R. E. Bonney, D. Fink, and S. Kelling (2009). eBird: A citizen-based bird observation network in the biological sciences. *Biological Conservation 142*(10), 2282–2292.

Taper, M. L. and P. J. P. Gogan (2002). The Northern Yellowstone elk: Density dependence and climatic conditions. *Journal of Wildlife Management 66*, 106–122.

Taylor, C. and D. R. Norris (2010). Population dynamics in migratory networks. *Theoretical Ecology 3*, 65–73.

Tucker, M. A., K. Böhning-Gaese, W. F. Fagan, J. M. Fryxell, B. Van Moorter, S. C. Alberts, A. H. Ali, A. M. Allen, N. Attias, T. Avgar, et al. (2018). Moving in the Anthropocene: Global reductions in terrestrial mammalian movements. *Science 359*(6374), 466–469.

Visser, M. E., A. C. Perdeck, J. H. van Balen, and C. Both (2009). Climate change leads to decreasing bird migration distances. *Global Change Biology 15*(8), 1859–1865.

Wiederholt, R., B. J. Mattsson, W. E. Thogmartin, M. C. Runge, J. E. Diffendorfer, R. A. Erickson, P. Federico, L. López-Hoffman, J. M. Fryxell, D. R. Norris, et al. (2018). Estimating the per-capita contribution of habitats and

pathways in a migratory network: a modelling approach. *Ecography 41*(5), 815–824.

Wikelski, M. and R. Kays (2019). Movebank: Archive, analysis and sharing of animal movement data. accessed on 25 Jan 2019.

Wilcove, D. and M. Wikelski (2008). Going, going, gone: Is animal migration disappearing? *PLoS Biology 6(7)*, e188.

Zamberletti, P., M. Zaffaroni, F. Accatino, I. F. Creed, and C. De Michele (2018). Connectivity among wetlands matters for vulnerable amphibian populations in wetlandscapes. *Ecological Modelling 384*, 119–127.